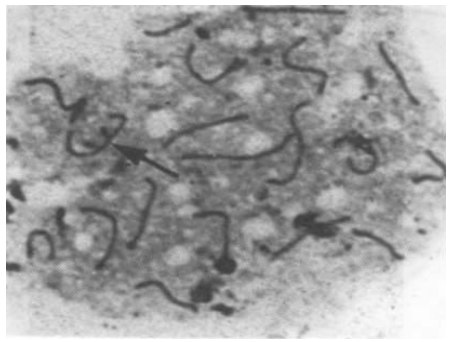

Fig. 4 Silver-stained light microscopic preparation of a pachytene mouse spermatocyte ($Rb7/t^{w5}$) displaying synaptonemal complexes of different lengths. Arrow indicates early disjunction of chromosomes 16 and 17 at the paracentromeric region. The preparation was according to ref. 17. ×1,430.

chromosomes 16 and 17 occurs in the presence of the *t* haplotype. This phenomenon may be related to the *t* haplotype and not to *Rb7*, because early disjunction does not occur in the *T/Rb7* sibling controls. Our electron microscopic studies also support the assumption of Lyon *et al.*[7] that chiasma suppression in *t* haplotypes results from normal synapsis without chiasma formation (desynapsis).

Artzt, Shin and Bennett have found an anomalous position of *H-2* with respect to *tufted* and *t*-haplotype lethality in t^{w5}, one of the *t* haplotypes used in this study[13]. The position could be most readily explained by an inversion of chromosome 17. Such inversions have not previously been found. Our electron microscopic and silver-staining studies of synaptonemal complexes have shown no evidence of inversions in either t^{w5} or t^{12}. As the *t* complex may extend for about 15 centimorgans, inversion loops would be expected if they were of this size—inversion loops of synaptonemal complexes were found in 100% of inversion carriers at early stages of meiosis[20]. Alternatively, the apparent change of position of *H-2* in these *t* alleles could represent expression of previously unexpressed type 1 histocompatibility antigen loci—recent evidence suggests much greater dispersion of type 1 loci, for at least several centimorgans, than had previously been expected[21]. Despite the central nce of crossing-over suppression for an understanding of the *t* complex, our electron microscopic analysis of synaptonemal complexes has not shown any clear-cut abnormalities. Thus, the final resolution of the enigma of the *t* complex must await the availability of DNA clones of the region.

Although our studies do not reveal the mechanism of *t*-allele-mediated cross-over suppression, further chromosomal studies are warranted as cross-over suppression and transmission ratio distortion in males, not embryonic lethality, are the truly unique properties of the *t* complex. The frequency of developmental lethals is probably no greater than expected in 15 centimorgans of DNA—the cross-over suppression maintains a block of DNA which can accumulate lethals and the unique population-selection properties of the *t* complex outbalance the loss due to homozygous lethality[22]. Recent discoveries of novel *t* alleles in novel complementation groups[23] suggest that previous developmental descriptions, based on a small number of complementation groups, have given a mistaken notion of molecular relatedness among these developmental lethals. Thus, all *t* lethals, and not just t^{w73} (ref. 24), may be 'parasitic'.

This work was supported by NIH grants HD 11738 and HD 11884.

Received 26 July; accepted 7 September 1982.

1. Dobrovalskaia-Zovadskaia, N. *C. r. Séanc. Soc. Biol.* **97**, 114–116 (1927).
2. Gluecksohn-Waelsch, S. & Erickson, R. P. *Curr. Topics dev. Biol.* **5**, 281–316 (1970).
3. Bennett, D. *Cell* **6**, 441–454 (1975).
4. Erickson, R. P., Hammerberg, C. & Sanchez, C. in *Current Research Trends in Prenatal Craniofacial Development* (eds Pratt, R. & Christiansen, R.) 103–117 (Elsevier, New York, 1980).
5. Forejt, J. *Folia biol.* **18**, 161–170 (1972).
6. Forejt, J. & Gregorova, S. *Cytogenet. Cell Genet.* **19**, 159–179 (1977).
7. Lyon, M. F., Evans, E. P., Jarvis, S. E. & Sayers, I. *Nature* **279**, 38–42 (1979).
8. Lyon, M. F. & Meredith, R. *Heredity* **19**, 301–312 (1964).
9. Lyon, M. F. & Meredith, R. *Heredity* **19**, 313–325 (1964).
10. Lyon, M. F. & Bechtol, K. B. *Genet. Res.* **30**, 63–76 (1977).
11. Erickson, R. P., Lewis, S. E. & Slusser, K. S. *Nature* **274**, 163–164 (1978).
12. Artzt, K., McCormick, P. & Bennett, D. *Cell* **28**, 463–470 (1982).
13. Artzt, K., Shin, H.-S. & Bennett, D. *Cell* **28**, 471–476 (1982).
14. Geyer-Duszynska, I. *Chromosoma* **15**, 478–502 (1964).
15. Womack, J. E. & Roderick, T. H. *J. Hered.* **65**, 308–310 (1974).
16. Dev, V. G. *et al. Genetics* **72**, 541–543 (1972).
17. Tres, L. L. & Kierszenbaum, A. L. in *Bioregulators of Reproduction* (eds Jagiello, G. & Vogel, H. J.) 229–256 (Academic, New York, 1981).
18. Tres, L. L. *J. Cell Sci.* **25**, 1–15 (1977).
19. Elder, F. F. B. & Pathak, S. *Cytogenet. Cell Genet.* **27**, 31–38 (1980).
20. Poorman, P. A., Moses, M. J., Davisson, M. T. & Roderick, T. H. *Chromosoma* **83**, 419–429 (1981).
21. Steinmetz, M., Winoto, A., Minard, K. & Hood, L. *Cell* **28**, 489–498 (1982).
22. Lewontin, R. C. & Dunn, L. C. *Genetics* **45**, 705–722 (1960).
23. Guenet, J.-L., Condamine, H., Gaillard, J. & Jacob, F. *Genet. Res.* **36**, 211–217 (1980).
24. Babiarz, B., Garrisi, G. J. & Bennett, D. *Genet. Res.* **39**, 111–120 (1982).

Cooperative motion and hydrogen exchange stability in protein β-sheets

F. R. Salemme*

Department of Molecular Biophysics and Biochemistry, Yale University, New Haven, Connecticut 06511, USA

Protein molecules are dynamical structures due to the continual exchange of thermal energy between them and the solvent environment[1,2]. This dynamic behaviour is manifest in hydrogen exchange experiments, which reflect transient solvent accessibility of groups usually buried in the protein interior[3,4]. However, studies of hydrogen exchange kinetics in pancreatic trypsin inhibitor (PTI) reveal a small subset of amide protons which exchange very slowly[5,6]. Four of these groups form successive interchain hydrogen bonds in the central region of an antiparallel β-sheet[7] (Fig. 1). Here I suggest that the unusual exchange stability of these β-sheet protons reflects the structure's intrinsic flexibility. This property allows transient energy fluctuations to be accommodated as cooperative motions which do not locally strain the interchain hydrogen bonds.

Observed hydrogen exchange rates for proteins typically span several orders of magnitude[3], which may reflect both intrinsic and environmental differences among the individual exchanging groups[8,9], as well as their static or dynamic accessibility to solvent molecules[4]. Nevertheless, examination of either the geometries[7,10] or solvent accessibilities[11] of the PTI sheet hydrogen bonds suggests little apparent reason why protons in the centre of the sheet should exchange more slowly than other similarly inaccessible groups (Fig. 1). Indeed, the data suggest that whatever the amplitude of dynamical motions in the fluctuating molecule[1,2], the central-sheet hydrogen bonds rarely break, as required to make them both accessible to, and reactive with, an exchanging water molecule[3,4,9].

Features of the antiparallel β-sheet which give rise to its flexibility are illustrated in Fig. 2, which shows a double-stranded sheet with linear N—H—O—C interchain hydrogen-bonds[12] (conformation 1 on the ϕ, ψ plot of Fig. 3). The structure can be viewed as a set of interconnected large and small hydrogen-bonded rings, each of which possesses a local dyad symmetry axis owing to the antiparallel sense of the polypeptide chains. This 'classical' structure can be continuously compressed in accordion-like manner so that it retains its symmetry properties[13]. This involves equivalent alteration in all the backbone ϕ, ψ angles and isoenergetic bending of the hydrogen-bonds[12,13] at the carbonyl oxygens (that is, conformations 1–4 in Fig. 3). Similarly, each flat sheet conformation can twist to

* Present address: Department of Biochemistry, University of Arizona, Tucson, Arizona 85721, USA.

0028–0836/82/420754—02$01.00

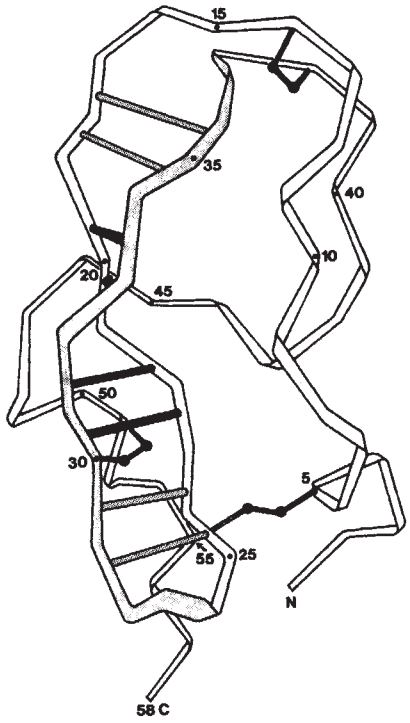

Fig. 1 A ribbon drawing of pancreatic trypsin inhibitor emphasizing the double-helical, antiparallel β-sheet (shaded) incorporating residues 17–36. Of the groups forming interchain hydrogen bonds in the sheet (illustrated as rungs interconnecting the polypeptide chain), four in the centre of the sheet (solid rungs) incorporate peptide amide groups which are unusually resistant to exchange with solvent protons, whereas those at the sheet ends exchange much more rapidly. Nevertheless, due to packing interactions of amino acid side chains, all the sheet hydrogen-bonding groups are similarly inaccessible to solvent in the crystal structure (for example, see Fig. 9 of ref. 13).

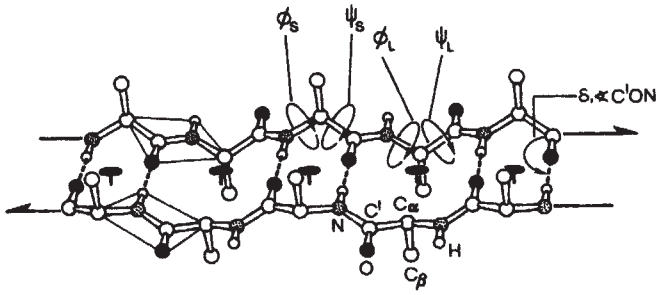

Fig. 2 A section of antiparallel β-sheet. The flat structure consists of 2-fold helical polypeptide chains linked by interchain hydrogen bonds. Due to the antiparallel N to C sense of the chains, the extended structure is organized as an interconnected array of 'small' and 'large' hydrogen-bonded rings, each of which has a 2-fold rotational symmetry axis normal to the mean sheet plane. The principal low-energy degrees of freedom of the backbone structure are torsional rotations about covalent backbone single bonds (ϕ_S, ψ_S, ϕ_L, ψ_L), and hydrogen-bond bending at the peptide carbonyl oxygen (δ).

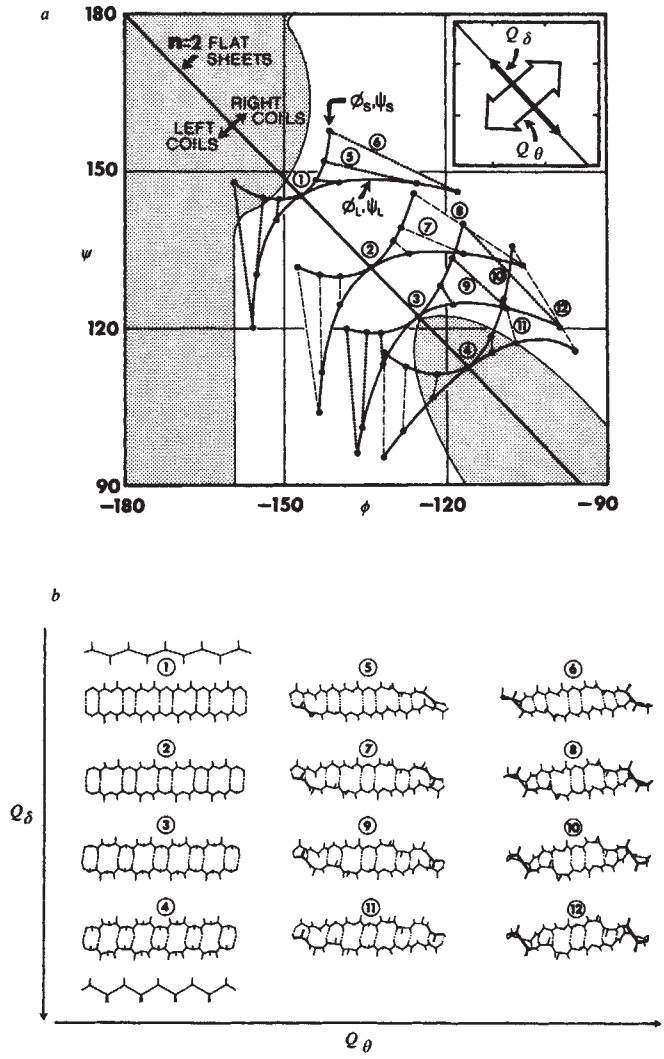

Fig. 3 *a* Shows the extended chain region of the ϕ, ψ plot. Various flat sheets are composed of 2-fold helical polypeptide chains having identical ϕ, ψ values for all residues. A continuum of flat-sheet conformations lie along the $n = 2$ line of the plot and differ in their hydrogen-bond bend angles (δ in Fig. 2), as shown by corresponding numbered structures in *b*. Any flat structure can cooperatively twist to form double-helical structures. This involves different, but correlated alterations in the ϕ, ψ angles of residues situated in small and large rings of the sheet. The twisted structures shown in *b* therefore consist of residues whose ϕ, ψ values alternate so that small ring residues all have conformational values ϕ_S, ψ_S, and large ring values ϕ_L, ψ_L, corresponding, respectively, to pairs of ϕ, ψ values connected by dashed and dotted lines in *a*. Shaded regions in *a* approximately delineate sterically disallowed sheet conformations. The accordion compression (Q_δ) and coiling (Q_θ) motions can be viewed as cooperative oscillation modes of the structure as a whole. Analysis of the potential energy surface[15] governing the coupled oscillations of the twisted sheet is consistent with a structure of unusual conformational flexibility.

form right-handed double-helical structures, corresponding to minimum energy conformations for extended polypeptide chains of L-amino acids[14,15]. In this case the chains coil so that the ϕs and ψs of residues in small and large hydrogen-bonded rings behave in a different, but correlated fashion. This double-helical coiling again preserves the ring symmetry in the structure, and equivalently, the interchain hydrogen bonds[13]. Due to the independence of the 'accordion' and coiling motions, the structure can undergo continuous interconversion between any of the structures shown in Fig. 3 via correlated motions associated with hydrogen-bond preservation. This reflects an extraordinary extent of conformational flexibility for an extended protein secondary structure. For example, comparable concerted ϕ, ψ excursions severely deform or sever the hydrogen-bonds in an α-helix[16].

As described elsewhere[13], the crystallographically observed[7] β-sheet in PTI is well approximated as a symmetrical and highly twisted structure of the type shown in Fig. 3. The observed structure therefore approximates a time-average superposition of the cooperative coiling (Q_θ) and accordion (Q_δ) motions, undergoing small excursions about their potential minima. Consequently, it might be anticipated that the same cooperative

interactions apparent in the crystallographic structure are retained when the molecule undergoes infrequent, larger fluctuations in energy. This suggests that fluctuations which might otherwise result in local structural disruptions promoting hydrogen exchange[3,4,8], can be accommodated in concerted β-sheet motions which incur little dynamic stress on the interchain hydrogen bonds.

As outlined above (see Fig. 3), the flexibility of the antiparallel β-sheet is a fundamental reflection of its symmetry properties, which allow equivalent preservation of the interchain hydrogen bonds for large cooperative displacements in its lowest-energy, torsional degrees of freedom (that is, ϕ, ψ rotations). However, the PTI sheet differs from the idealized model as the strands are interconnected by a β-turn at one end, and sharply folded over at the other (Fig. 1). In the present context, these interactions at the sheet ends can be viewed as imposing constraints on symmetrical oscillations characterizing the remainder of the structure. In other words, excursions in the symmetrical modes would be expected to localize dynamic stresses, and hence frequently break hydrogen bonds, at the sheet ends, where the structure deviates most from the idealized symmetry. This behaviour is consistent with the observed exchange properties in PTI, where the hydrogen bonds at the sheet ends (Fig. 1) exchange much faster than those in the centre[5,6].

Although dynamical simulations[17,18] of PTI cover time intervals many orders of magnitude shorter than that generally associated with hydrogen exchange processes[3], they show properties consistent with the behaviour described here. Specifically, these simulations give evidence for both correlated oscillations about the β-sheet backbone bonds[17] and preservation of the interchain hydrogen bonds in the sheet centre[18]. Figure 3 illustrates that these properties are retained even during infrequent fluctuations, resulting in significant displacements from the structure's minimum free energy state.

These observations suggest that the unusual exchange stability observed in the PTI β-sheet, and also seen in more extended antiparallel sheets in trypsin[19] and ribonuclease[20], reflects cooperative oscillations in these structures as a whole. Such cooperative motions may be relevant to protein folding, stabilization and function[21]. For example, the coupled motions described suggest highly cooperative pathways for β-sheet folding. Similarly, oscillations in the folded structure, corresponding to thermal excitation of low-frequency vibrational modes[21], may contribute a favourable vibrational entropy component to the molecule's stabilization free energy[22]. Finally, these cooperative motions are ordered both in space and time, features implicit in most present proposals for enzyme allostery and mechanism.

I thank F. M. Richards and M. Karplus for helpful discussions. This work is supported by NIH grant GM-21534.

Received 24 May; accepted 9 August 1982.

1. Careri, G., Fasella, P. & Gratton, E. *A. Rev. Biophys. Bioengng* **8**, 69–97 (1979).
2. Cooper, A. *Proc. natn. Acad. Sci. U.S.A.* **73**, 2740–2741 (1976).
3. Englander, S. W., Downer, N. W. & Teitlebaum, H. *A. Rev. Biochem.* **41**, 903–924 (1972).
4. Richards, F. M. *Carlsberg Res. Commun.* **44**, 47–63 (1979).
5. Wuthrich, K. & Wagner, G. *J. molec. Biol.* **150**, 1–18 (1979).
6. Wagner, G. & Wuthrich, K. *J. molec. Biol.* **134**, 75–94 (1979).
7. Deisenhofer, J. & Steigemann, W. *Acta crystallogr.* B**31**, 238–251 (1975).
8. Molday, R. S., Englander, S. W. & Kallen, R. G. *Biochemistry* **1**, 150–158 (1972).
9. Eigen, M. *Angew. Chem. int. Edn. Engl.* **3**, 1–72 (1964).
10. Hagler, A. & Lifson, S. in *Peptides, Polypeptides and Proteins* (eds Blout, E., Bovey, F., Goodman, N. & Lotan, N.) 35–48 (Wiley Interscience, New York, 1974).
11. Lee, B. & Richards, F. M. *J. molec. Biol.* **55**, 379–400 (1971).
12. Pauling, L. & Corey, R. *Proc. natn. Acad. Sci. U.S.A.* **37**, 729–740 (1951).
13. Salemme, F. R. & Weatherford, D. W. *J. molec. Biol.* **146**, 119–121 (1981).
14. Ramachandran, G. in *Peptides, Polypeptides and Proteins* (eds Blout, E., Bovey, F., Goodman, M. & Lotan, N.) 14–34 (Wiley Interscience, New York, 1974).
15. Raghavandra, K. & Sasisekharan, V. *Int. J. Peptide Protein Res.* **14**, 326–338 (1979).
16. Levy, R. M. & Karplus, M. *Biopolymers* **18**, 2465–2495 (1979).
17. McCammon, J. A., Gelin, B. R. & Karplus, M. *Nature* **277**, 585–590 (1977).
18. Levitt, M. *Nature* **294**, 379–380 (1981).
19. Kossiakoff, A. A. *Nature* **296**, 713–721 (1982).
20. Wlodawer, A. & Sjolin, L. *Proc. natn. Acad. Sci. U.S.A.* **79**, 1418–1422 (1928).
21. Peticolas, W. L. *Meth. Enzym.* **61**, 425–456, (1979).
22. Sturtevant, J. M. *Proc. natn. Acad. Sci. U.S.A.* **74**, 2236–2240 (1977).

Redesigning enzyme structure by site-directed mutagenesis: tyrosyl tRNA synthetase and ATP binding

Greg Winter*, Alan R. Fersht†, Anthony J. Wilkinson†, Mark Zoller‡ & Michael Smith‡

*MRC Laboratory of Molecular Biology, Hills Road, Cambridge CB2 2QH, UK
†Department of Chemistry, Imperial College of Science and Technology, London SW7 2AY, UK
‡Department of Biochemistry, Faculty of Medicine, University of British Columbia, 2146 Health Sciences Mall, Vancouver, British Columbia, Canada V6T 1W5

We describe here a general method for systematically replacing amino acids in an enzyme. This allows analysis of their molecular roles in substrate binding or catalysis and could eventually lead to the engineering of new enzymatic activities. The gene encoding the enzyme is first cloned into a vector from which the enzyme is expressed and is then mutated *in vitro* to change a particular nucleotide and hence the amino acid sequence of the enzyme. We have cloned the gene for the tyrosyl tRNA synthetase of *Bacillus stearothermophilus* into a vector derived from the single-stranded bacteriophage M13 to facilitate mutagenesis with mismatched synthetic oligodeoxynucleotide primers. From the recombinant M13 clone we have obtained high levels of the enzyme (~50% of soluble protein) expressed in the *Escherichia coli* host and have converted cysteine (Cys 35) at the enzyme's active site to serine. This leads to a reduction in enzymatic activity that is largely attributable to a lower K_m for ATP.

The tyrosyl tRNA synthetase (TyrTS) catalyses the aminoacylation of $tRNA^{Tyr}$ with tyrosine by a two-step mechanism in which tyrosine is first activated by ATP to form tyrosyl adenylate and then transferred to $tRNA^{Tyr}$ (refs 1, 2). The nucleotide sequence of the gene has been determined from a clone in the plasmid vector pBR322[3] and the enzyme is expressed in *E. coli* from its own promoter to about 10% of total soluble protein[4]. X-ray crystallographic analysis of the tyrosyl enzyme is complete to ~3 Å resolution[5] and the binding sites of tyrosine and ATP have been identified[6,7]. The target for mutagenesis was Cys 35[8], which is also present in the structures of the tyrosyl and methionyl tRNA synthetases of *E. coli*[9]. In the crystallographic model of the tyrosyl enzyme, this residue makes a contact with the 3′ hydroxyl of the sugar moiety of tyrosyl adenylate, possibly via a hydrogen bond (D. Blow, personal communication). We decided to replace this cysteine by serine, a close structural analogue, expecting that a conservative change in a binding contact might alter, but not destroy, enzyme activity.

Initially the gene encoding the tyrosyl tRNA synthetase and its promoter were re-cloned from pBR322[4] into the single-stranded bacteriophage M13 to facilitate mutagenesis[10] (Fig. 1). The principle of oligonucleotide-directed mutagenesis relies on the extension of a primer by DNA polymerase (large fragment on a single-stranded circular template[11–24]. The primer, 5′ CAAACCCGCTTGTAGAG 3′, was complementary to the template except for a single internal mismatch (*) which directs the mutation Cys (TGC) to Ser (AGC). The mismatch is sited in the middle of the primer to protect it from exonuclease action and the precise sequence and length of the primer was chosen to minimize spurious matches elsewhere in the gene or in M13. The newly synthesized strand was sealed with ligase and *E. coli* cells transfected with the cloned circular double-stranded molecule.

0028–0836/82/420756—02$01.00